Forest Fire Detection in the Ethiopian Highlands Using Remote Sensing Data

Ammanuel Hailye, Xingdong Wang*, Yuhua Wang**

College of Information Science and Engineering，Henan University of Technology，Zhengzhou 45001，China

Abstract: *Forest fires are a recurring environmental hazard in the Ethiopian Highlands, endangering biodiversity, local communities, and the ecosystem. In regions like the Ethiopian Highlands, forest loss also disrupts local climate regulation, potentially leading to extreme weather events such as droughts and landslides. Therefore, this study utilizes remote sensing data from 2016-2024 to detect and analyze forest fires in the Ethiopian Highlands, focusing on improving dNBR thresholds. We developed an algorithm using a Python interface that computes by integrating dNBR binarized image with terrain aspect for enhanced detection, incorporating Otsu's method and morphological operations on dNBR extractions to improve accuracy. In this study, the improved dNBR threshold based on the terrain aspect algorithm is compared to the previous standard dNBR thresholding method, and the results clearly show that the high fire-prone regions can be obtained with the improved method. Findings are essential for protecting ecosystems, informing reforestation, and segmenting high-severe fire areas.*

Keywords: *Forest fires, Ethiopian Highlands, Remote sensing, Satellite imagery, Fire detection, dNBR*

I. Introduction

Remote sensing technologies have transformed forest fire detection, allowing for efficient monitoring of vast areas, especially where ground access is limited. The study area, East Benishangul-Gumuz Wildlife Protection Park, lies in northwestern Ethiopia. This extensive ecological zone covers approximately 50,381 km², with an elevation of 1200–1500 meters above sea level and annual temperatures ranging between 20–40°C. The park, situated between latitudes 9°17'–12°06' N and longitudes 34°04'–37°04' E, supports a variety of ecosystems, with diverse vegetation and wildlife (Fig 1).

Satellite platforms such as MODIS (Moderate Resolution Imaging Spectroradiometer), VIIRS (Visible Infrared Imaging Radiometer Suite), and Landsat play vital roles in both real-time fire detection and post-fire assessment. While these sensors excel at large-scale monitoring, limitations exist, especially with small or low-intensity fires. Higher-resolution data from platforms like Landsat-8 is often required for detailed post-fire damage assessment. The dNBR (differenced Normalized Burn Ratio) index, introduced by Key and Benson (1999), has become a standard for estimating burn severity by comparing pre- and post-fire satellite imagery. Although widely effective in assessing large fires, especially in North America and Europe, dNBR thresholds require adjustment to align with local ecological characteristics for accurate interpretations of burn severity [1].

Effective fire detection relies heavily on optimal thresholding of remote sensing indices. One common method, Otsu's algorithm, automatically selects the optimal threshold to differentiate between burned and unburned areas. Studies, such as those by Gao, Zhou, and Wang (2020) in Liangshan, China, have demonstrated the effectiveness of Otsu's algorithm using Landsat-8 data to delineate fire-affected regions. However, they emphasized that further advancements in thresholding methods could improve accuracy [2]. Similarly, Giglio et al. (2016) explored fire radiative power (FRP) and active fire detection using MODIS and VIIRS, finding that while these data are valuable for initial detection, local environmental conditions must be incorporated into threshold values to reduce false positives in complex terrains like the Ethiopian Highlands [3].

Research on African ecosystems provides valuable insights into fire dynamics and the unique challenges of remote sensing in this region. Archibald et al. (2013) analyzed fire regimes across African savannas, emphasizing the combined impact of natural and human activities on fire occurrences. Their study highlighted the seasonal nature of fires, particularly during dry periods, underscoring the need for refined fire management strategies [4]. Bastarrika, Chuvieco, and Martín (2011) developed a MODIS-based fire detection

method for tropical savannas, noting that while dNBR is effective, regional calibration is essential, especially in mixed-vegetation areas like the Ethiopian Highlands [5]. Other studies, including Miller et al. (2009), have shown that dNBR thresholds for temperate forests are not directly applicable to diverse ecosystems, reinforcing the need for region-specific calibration [6].

Despite extensive global research on fire detection, few studies have concentrated specifically on the Ethiopian Highlands. Existing detection models often rely on thresholds developed for other ecosystems, which may not account for the Highlands' unique climate, topography, and vegetation. For instance, dNBR thresholds may not fully capture fire severity variations here, potentially leading to inaccurate estimates of burned areas. Moreover, limited research has examined the influence of seasonal changes on fire detection in this region. Archibald et al. (2010) highlighted the role of seasonal cycles in African fire dynamics, yet similar research specific to the Ethiopian Highlands remains sparse [7].

In summary, remote sensing indices like dNBR have proven globally effective in fire detection, but region-specific adaptations are essential for accurate application in the Ethiopian Highlands. This study addresses this need by enhancing the dNBR threshold method with terrain aspect factors to improve accuracy. Additionally, understanding seasonal influences on fire behavior in the Ethiopian Highlands presents a significant opportunity for future research.

II. Data and Methods

2.1 Principles and methods

This study employed the differenced Normalized Burn Ratio (dNBR) method to extract fire-affected areas through spectral analysis of satellite imagery before and after fire events. dNBR leverages the spectral reflectance in the Near-Infrared (NIR) and Short-Wave Infrared (SWIR) bands to quantify burn severity [8]. For this method, the Normalized Burn Ratio (NBR) is calculated independently for pre-fire and post-fire images using the formula:

$$NBR = \frac{NIR - SWIR}{NIR + SWIR} \qquad (1)$$

The dNBR is then computed by subtracting the post-fire NBR from the pre-fire NBR, resulting in positive values for burned areas indicating high burn severity and near-zero or negative values for unburned areas [9].

To improve the standard dNBR method, we employed an aspect-specific dNBR adjustment, refining fire severity mapping by modifying thresholds based on terrain aspect. This approach leverages research by Holden et al. (2005) and Key and Benson (2006) on how terrain influences burn severity through variations in sunlight exposure and vegetation dryness [9][10]. This method introduces an adjustment factor to the base threshold based on aspect, using the formula:

$$Adjusted\ threshold\ =\ base\ threshold\ *\ (1\ +\ aspect\ factor) \qquad (2)$$

Where: the aspect factor modifies the base threshold according to terrain aspect to account for increased solar exposure and vegetation dryness. For example, south-facing slopes, which receive more direct sunlight, may require a higher threshold adjustment, while north-facing slopes, with reduced exposure, have lower adjustments. This aspect-informed adjustment allows for a more precise delineation of fire severity, especially in complex terrains, enhancing model accuracy in regions like the Ethiopian Highlands.

2.2 Data collection process

In this study we used Landsat 8 OLI_TIRS and SRTM DEM satellite data. These data were downloaded from the archives of the United States Geological Survey (USGS), accessed through the Earth Explorer interface. We obtained Landsat 8 images from 2016 to 2024 (WRS-2 path/row 170/53), pre-fire (Wet season) and post fire (Dry season) data. After we collect the data, first we preprocess the remote sensing data for both periods to correct for atmospheric effects, radiometric calibration, and geometric corrections. This ensures that the data is suitable for analysis. The study regions are shown in Fig 1.

a   b
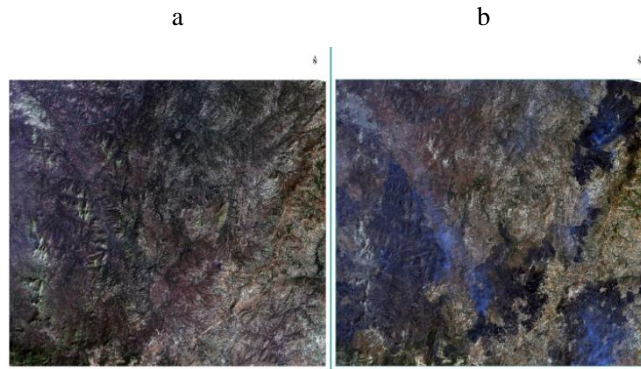
Fig.1 Study regions (a)pre-fire, (b)post fire

The main workflow for aspect specific dNBR thresholding for fire area extraction is showed in Fig 2.
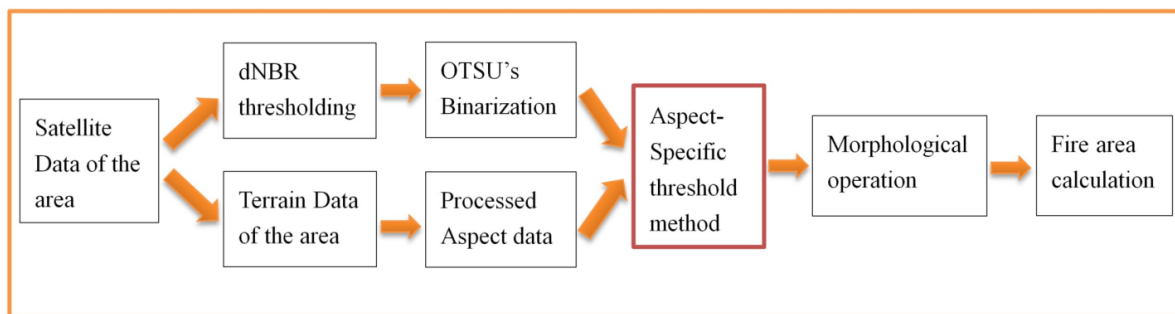
Fig.2 Forest fire extraction process

Accurate fire detection depends heavily on effective thresholding of remote sensing indices. Otsu's algorithm, which automatically selects the optimal threshold for separating two classes burned vs. unburned areas, has been a common approach. Gao, Zhou, and Wang (2020) applied this method in their study of forest fires in Liangshan, China [2]. The main workflows for our study image processing steps are clearly shown in Fig 2. The image processed into dNBR thresholding method, then OTSU's binarization method, side by side we process the terrain aspect of the region, and then by incorporating with terrain data a new aspect specific threshold image obtained and finally morphological opening operation for image enhancement. After these steps we can clearly observe the fire area for further analysis.

III.   Remote sensing data processing

3.1 dNBR image processing

In the case of Landsat 8, band 5 (0.85-0.88 μm) and band 7 (2.11-2.29 μm). NBR is calculated as: (Band5 – Band7) / (Band 5 + Band7). The values before the fire range from 0.22 to 0.58. These values are generally positive, indicating unburned vegetation. NBR values after the fire range from -0.28 to 0.50. Areas with negative values typically indicate burned regions. The results are showed below Fig 3.

a   b
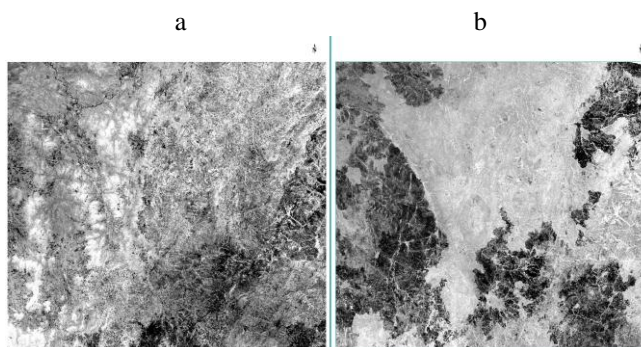
Fig.3 NBR before fire and NBR after fire images.

Then next we can calculate the dNBR value by subtracting the post-fire NBR from the pre-fire NBR:

$$dNBR = pre\_NBR - after\_NBR \qquad (3)$$

With burned areas appearing as bright spots compared to the surrounding areas. The resulting range of the dNBR values is -0.23 to 0.57. The result is showed below Fig 4.
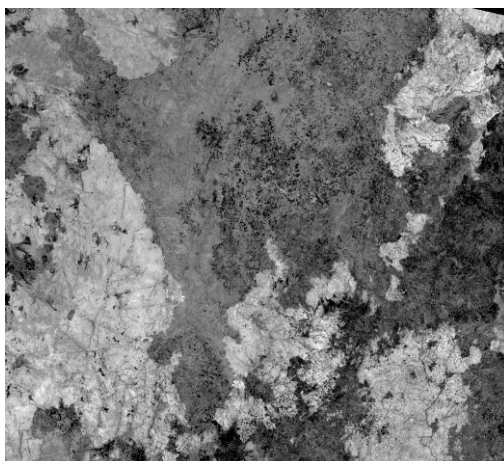
Fig.4 dNBR Difference Image

3.2 OTSU's Thresholding

Otsu's algorithm involves the following steps:

First step: Convert the normalized image to a grayscale image, if it's not already.

Second step: Compute the histogram of the grayscale image. This histogram is the core of Otsu's method, representing the distribution of pixel intensities across possible threshold values. A well-separated histogram (bimodal) typically indicates that the image can be easily segmented into two classes, background and foreground [11][12][13]. These studies highlight that when dNBR or other indices are used, the histogram can display clear peaks corresponding to burned and unburned regions, making histogram-based methods like Otsu's effective.

Third step: Traverse through all possible threshold values (0 to 255) and calculate the between-class variance for each threshold. The algorithm divides the histogram into two classes at each threshold t: background (pixels with intensities from 0 to t) and foreground (pixels with intensities from t+1 to 255). For each threshold, the following parameters are computed: Within-class variance: This measures the spread of intensities within each class. Between-class variance: This measures the difference in intensity between the two classes. The goal is to identify the threshold that maximizes the between class variance, as this value indicates the most distinct separation between foreground and background pixels. This process is widely discussed in other studies [10][11][14][15].

Forth step: Select the threshold that minimizes the within-class variance (equivalently, maximizes the between-class variance). These steps are widely discussed and clearly shown in other studies. [11][16][17].

For the image that we're processing, the OTSU's Binarized image threshold value was 137 and the result of the processed image is showed below Fig 5.
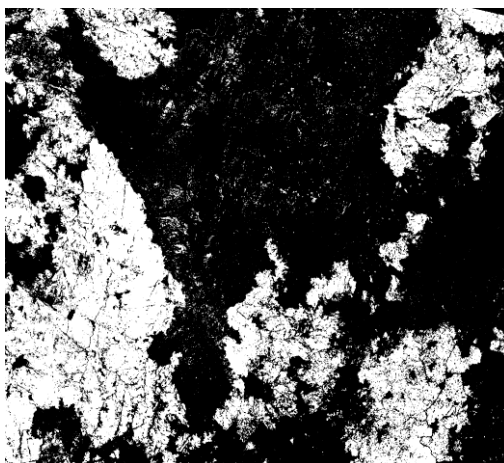
Fig.5 Otsu's threshold binarized dNBR image

3.3 Aspect-adjusted dNBR thresholding method

After we collect the SRTM DEM (Digital Elevation Model) data from satellite source we can process it to derive the aspect of each pixel within the study area. Aspect was extracted using GIS software, which calculates the compass direction (0–360°) of the slope for each pixel in the DEM. The result is showed below Fig 6.
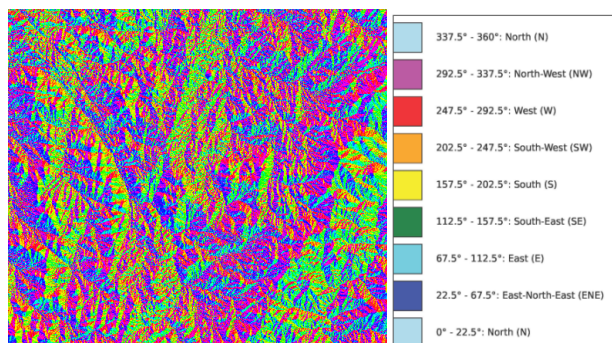
Fig.6 Interpretation of land's aspect with different coloring and angle

The continuous aspect values were classified into categories representing general directional slopes: north-facing (0° to 45° and 315° to 360°), south-facing (135° to 225°), east-facing (45° to 135°), and west-facing (225° to 315°) [18].

After we input both the dNBR binarized image and the terrain aspect data into the algorithm, it calculates the new adjusted threshold, based on the aspect factor. Which is in our case, we adjust South-facing slopes (135° to 225°) by only +0.1 or an increase in 1%. Same wise North-facing slopes (0° to 45° and 315° to 360°) by only -2 or we adjusted the factor to decrease by 20%. And same wise 0 factor for East and West-facing slope. An algorithm that process by incorporating terrain-based adjustments which is Aspect, into dNBR thresholding allows for a more realistic and nuanced classification of fire severity. Result of the aspect based threshold image is showed on Fig.7
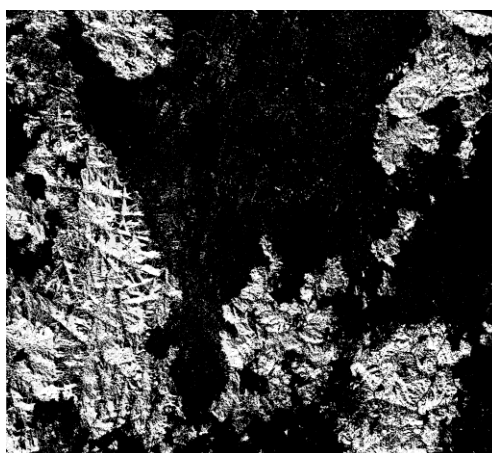
Fig.7 Aspect-adjusted dNBR result

3.4 Morphological operation

This process plays a significant role on enhancing a binarized image by removing small fragmented polygons. The morphological opening operation combines two basic operations: erosion and dilation. It uses a structuring element to first erode the image, removing small objects and noise and then dilates it to restore the size and shape of the remaining objects [19][20][21]. Erosion ($\ominus$): This operation shrinks the boundaries of objects in a binary image. It removes pixels on object boundaries, typically eliminating small details and noise. Dilation ($\oplus$): This operation expands the boundaries of objects in a binary image. It adds pixels to the boundaries of objects, typically filling in small holes and gaps [22]. This method follows this equation:

$$I \circ B = (I \ominus S) \oplus S \qquad (4)$$

Where: I is the input binarized image, S is the structuring element used for both erosion and dilation, $\ominus$ represents the erosion operation, $\oplus$ represents the dilation operation, B is the resulting image after applying the

opening operation. After we process the image through Morphological opening operation the result is shown on Fig.8.
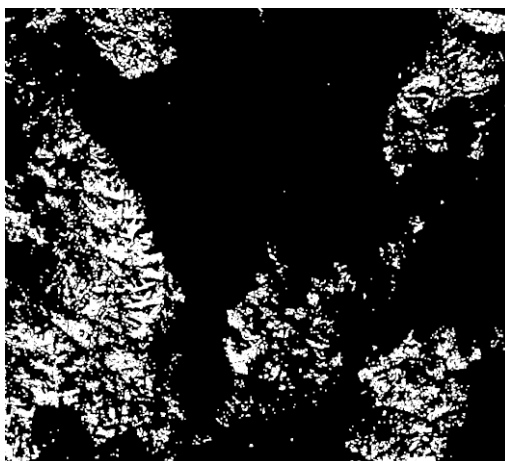
Fig.8 Morphological opening operation on aspect based dNBR binarized image result

IV. Data Evaluation

4.1 Comparison of Standard dNBR threshold to Aspect-adjusted dNBR threshold

We processed fire activity images spanning from 2016 to 2024 using both the standard differenced Normalized Burn Ratio (dNBR) method and the aspect-adjusted dNBR threshold method. Following these analyses, we conducted a comparative evaluation to determine if the aspect-based adjustments improved the accuracy of fire severity thresholds. As illustrated in Fig.9, the results highlight the areas with high fire severity, demonstrating the effectiveness of terrain-informed threshold adjustments in enhancing the precision of burn severity mapping.

(a)

(b)

(c)

(d)

(e)
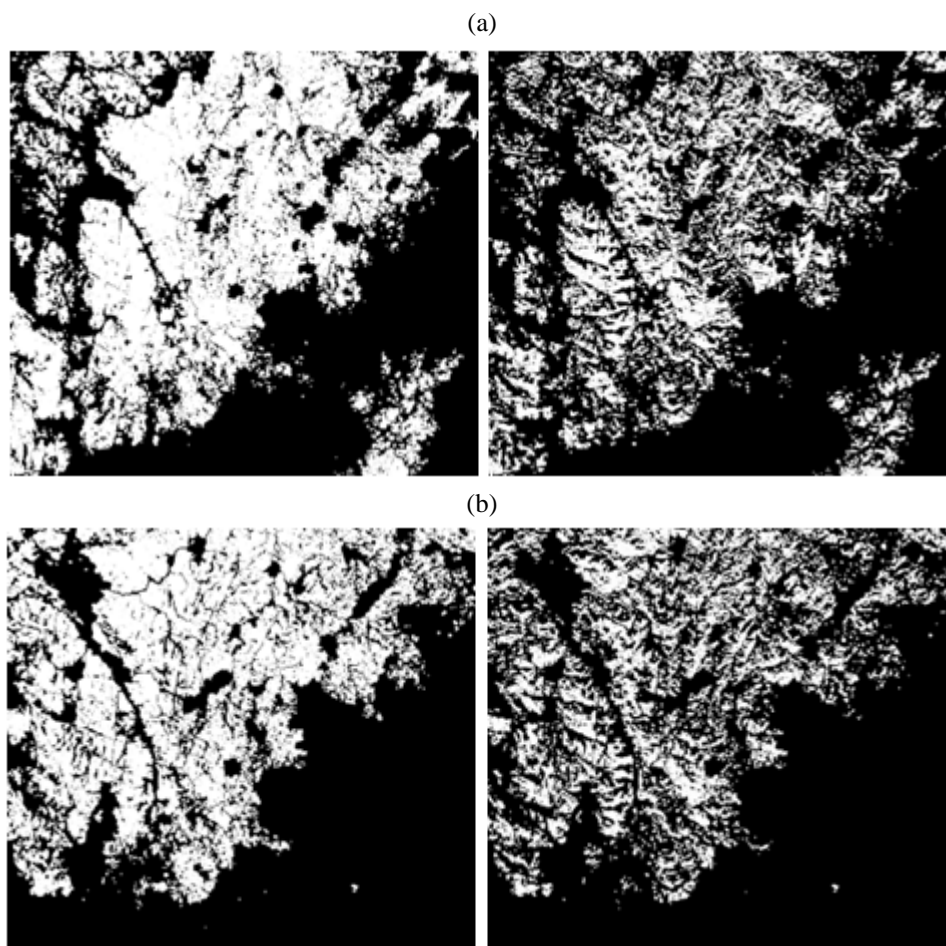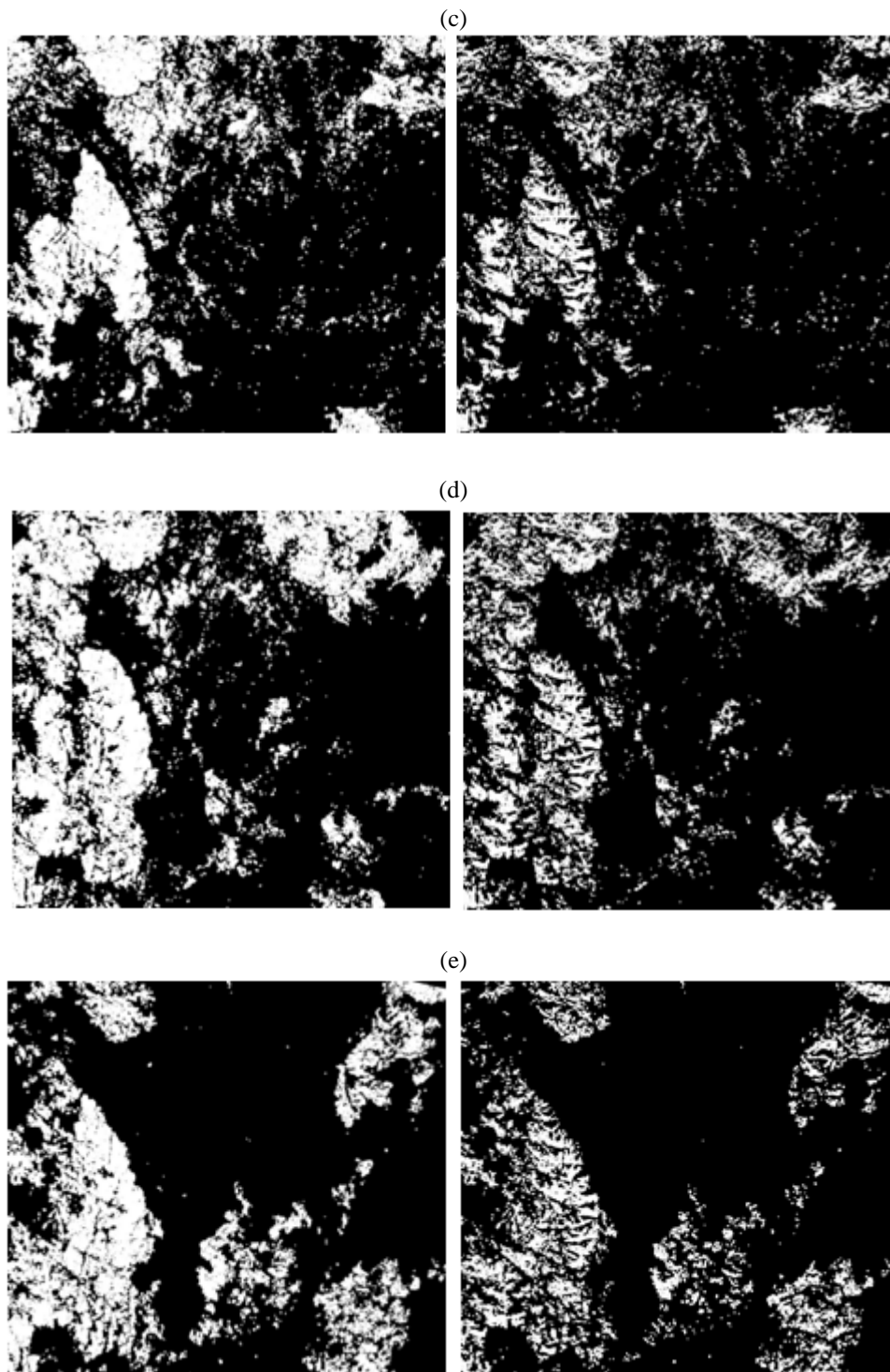
Fig.9 Standard dNBR threshold method and Aspect-adjusted dNBR threshold method results (a)2016-2018, (b)2019-2020, (c)2020-2021, (d)2022-2023, (e)2023-2024

Our evaluation reveals that incorporating terrain aspect into the thresholding process significantly improves the accuracy of burned area classification compared to the traditional dNBR threshold method. This terrain-aware adjustment provides a more refined distinction of burn severity across varying slopes. Specifically, our analysis shows that north-facing slopes, which receive less direct sunlight, retain higher moisture levels and exhibit cooler temperatures, leading to potentially less intense fire behavior. These areas were adjusted by a factor of -2, reducing the dNBR values by 20%. This adjustment reflects the expected lower fire severity in

these areas, as confirmed by their significantly lower adjusted dNBR values relative to other slopes. In contrast, south-facing slopes, with greater direct sunlight exposure, experience drier conditions that predispose them to more severe fire behavior. A minor adjustment factor of +0.1 (1%) was applied, acknowledging that these areas naturally exhibit high dNBR values due to increased aridity and heat. The minimal adjustment confirms that south-facing slopes maintain higher dNBR values, reinforcing their susceptibility to intense fires. East- and west-facing slopes, receiving moderate sunlight, were adjusted by a neutral factor of 1.0, indicating that their dNBR values were not significantly altered. The moderate fire behavior observed on these slopes aligns with expectations, placing their severity between that of north- and south-facing slopes. By adjusting dNBR values according to terrain aspect, we enhance the fidelity of fire severity maps, ensuring they accurately reflect the topographic influences on fire behavior. This approach improves threshold-based classifications for low, moderate, and high burn severity categories, enabling more precise identification of fire-affected areas.

In summary, aspect-informed dNBR adjustments advance the traditional thresholding method by integrating terrain factors, particularly aspect, into the classification process. This enhancement enables a more nuanced and accurate classification of fire severity across diverse topographies.

V. Fire area calculation and analysis

5.1 Fire Area calculation

After identifying the burned areas through the methods, the pixel count of burned areas is converted to area measurements in hectares. Since each Landsat 8 pixel represents 900 square meters, multiplying the pixel count by 900 and converting to appropriate units gives the total burned area. Therefore it can be calculated as follow: Burned Area (hectares) = Number of Burned Pixels * 0.09. We calculate the fire area by processing the remote sensing data using both standard dNBR thresholding method and aspect-adjusted dNBR threshold method. Through this analysis, we identify and quantify the most severely affected areas. This approach enhances the accuracy of burned area assessments by incorporating terrain influences, offering valuable insights for targeted post-fire recovery and management efforts.

5.2 Results analysis

The results from both the standard dNBR threshold method and the aspect-adjusted dNBR threshold method reveal important insights into the accuracy and effectiveness of incorporating terrain aspect in burn severity mapping. By comparing the fire-affected areas calculated in hectares (ha) for both methods, we gain a clearer understanding of how aspect influences fire severity classification. Table 1 showed the results for this analysis.

Table 1 Comparison of fire area between Standard dNBR Threshold and aspect-adjusted dNBR threshold method

Threshold Method	2016-2018	2019-2020	2020-2021	2022-2023	2023-2024
Standard dNBR Threshold fire area calculated (ha)	106.98	90.92	57.58	70.51	55.98
Aspect-adjusted dNBR Threshold fire area calculated (ha)	63.86	53.8	32.7	41.2	33.13

From the above table we can understand that the improved dNBR thresholding method consistently yields lower fire area calculations compared to the original dNBR thresholding method across all years. The reduction in calculated fire area with the improved method varies each year, suggesting that the improvement in thresholding effectively filters out non-burned areas or minimizes misclassification and miscalculation. While both methods show variations in fire area year-to-year, the improved method demonstrates a more conservative estimate, which could indicate higher accuracy in identifying truly fire areas.

VI. Conclusion

Therefore we can conclude that the aspect-adjusted dNBR threshold method appears to be more effective at delineating the high sever fire area occurred during 2016-2024 in the Ethiopian highlands, possibly due to factors such as refined adjustments for terrain or other environmental influences. This method reduces the overestimation of burned area seen with the standard dNBR threshold, likely by filtering out areas influenced by other factors specially terrain aspect factor. Furthermore aspect-adjusted dNBR threshold method is needed to improve its precision by incorporating additional terrain factors, such as slope and elevation, to further enhance dNBR thresholding accuracy.

References

[1] Key, C. H., & Benson, N. C. (1999). Measuring and remote sensing of burn severity: The CBI and NBR. In L.F. Neuenschwander & K.C. Ryan (Eds.), Proceedings of the Joint Fire Science Conference and Workshop (Vol. II, pp. 284-293). University of Idaho and the International Association of Wildland Fire.

[2] Gao, Y., Zhou, Y., & Wang, Y. (2020). Post-fire vegetation recovery and its driving factors in Liangshan, China, based on Landsat time series. International Journal of Applied Earth Observation and Geoinformation, 92, 102163.

[3] Giglio, L., Schroeder, W., & Justice, C. O. (2016). The collection 6 MODIS active fire detection algorithm and fire products. Remote Sensing of Environment, 178, 31-41.

[4] Archibald, S., Lehmann, C. E. R., Gómez-Dans, J. L., & Bradstock, R. A. (2013). Defining pyromes and global syndromes of fire regimes. Proceedings of the National Academy of Sciences, 110(16), 6442-6447.

[5] Bastarrika, A., Chuvieco, E., & Martín, M. P. (2011). Mapping burned areas from Landsat TM/ETM+ data with a two-phase algorithm: Balancing omission and commission errors. Remote Sensing of Environment, 115(4), 1003-1012.

[6] Miller, J. D., Safford, H. D., Crimmins, M., & Thode, A. E. (2009). Quantitative evidence for increasing forest fire severity in the Sierra Nevada and southern Cascade Mountains, California and Nevada, USA. Ecosystems, 12(1), 16-32.

[7] Archibald, S., Roy, D. P., Van Wilgen, B. W., & Scholes, R. J. (2010). What limits fire? An examination of drivers of burnt area in Southern Africa. Global Change Biology, 16(2), 606-619.

[8] Miller, J. D., & Thode, A. E. (2007). Quantifying burn severity in a heterogeneous landscape with a relative version of the delta Normalized Burn Ratio (dNBR). Remote Sensing of Environment, 109(1), 66-80.

[9] Key, C. H., & Benson, N. C. (2006). Landscape assessment: Remote sensing of severity, the Normalized Burn Ratio; and ground measure of severity, the Composite Burn Index.

[10] Holden, Z. A., Morgan, P., & Shlisky, A. J. (2005). Effects of terrain and aspect on fire severity in the western United States. Fire Ecology, 1(1), 11-22.

[11] Otsu, N. (1979). A threshold selection method from gray-level histograms. IEEE Transactions on Systems, Man, and Cybernetics, 9(1), 62-66.

[12] Fraser, R. H., Carver, G. D., & O'Neill, R. V. (2000). Remote sensing of fire severity and vegetation recovery. International Journal of Remote Sensing, 21(18), 3585-3601.

[13] Mitri, G., & Gitas, I. (2004). Fire severity mapping and vegetation recovery assessment using Landsat TM imagery: A case study from the Mediterranean region. International Journal of Remote Sensing, 25(19), 3803-3822.

[14] Sezgin, M., & Sankur, B. (2004). Survey over image thresholding techniques and quantitative performance evaluation. Journal of Electronic Imaging, 13(1), 146-168.

[15] Parks, S. A., Holsinger, L. M., Panunto, M. H., Jolly, W. M., Dobrowski, S. Z., & Dillon, G. K. (2018). High-severity fire: Evaluating its key drivers and mapping its probability across western US forests. Environmental Research Letters, 13(4), 044037.

[16] Sonka, M., Hlavac, V., & Boyle, R. (2008). Image processing, analysis, and machine vision (3rd ed.). Cengage Learning.

[17] Veraverbeke, S., Lhermitte, S., Verstraeten, W. W., & Goossens, R. (2011). Evaluating spectral indices and spectral mixture analysis for assessing fire severity, combustion completeness, and carbon emissions. International Journal of Wildland Fire, 20(5), 712-724.

[18] Keane, R. E., Holsinger, L. M., Parsons, R. A., & Gray, K. L. (2015). Climate change effects on historical range and variability of two large landscapes in western Montana, USA. Forest Ecology and Management, 351, 28-39.

[19] Serra, J. (1982). Image analysis and mathematical morphology. Academic Press.

[20] Gitas, I. Z., Mitri, G. H., & Ventura, G. (2004). Object-based image classification for burned area mapping of Creus Cape, Spain, using NOAA-AVHRR imagery. Remote Sensing of Environment, 92(3), 409-413.

[21] Fauvel, M., Benediktsson, J. A., Chanussot, J., & Sveinsson, J. R. (2006). Spectral and spatial classification of hyperspectral data using SVMs and morphological profiles. IEEE International Geoscience and Remote Sensing Symposium, 4, 2490-2493.

[22] Dougherty, E. R. (1992). An introduction to morphological image processing. SPIE Optical Engineering Press.